THE UNIVERSITY of EDINBURGH

Edinburgh Research Explorer

Widely tunable MEMS ring resonator with electrothermal actuation and piezoelectric sensing for filtering applications

Citation for published version:
Sviličić, B, Mastropaolo, E & Cheung, R 2015, 'Widely tunable MEMS ring resonator with electrothermal actuation and piezoelectric sensing for filtering applications', *Sensors and Actuators A: Physical*, vol. 226.
https://doi.org/10.1016/j.sna.2015.02.023

Digital Object Identifier (DOI):
10.1016/j.sna.2015.02.023

Link:
Link to publication record in Edinburgh Research Explorer

Document Version:
Peer reviewed version

Published In:
Sensors and Actuators A: Physical

General rights
Copyright for the publications made accessible via the Edinburgh Research Explorer is retained by the author(s) and / or other copyright owners and it is a condition of accessing these publications that users recognise and abide by the legal requirements associated with these rights.

Take down policy
The University of Edinburgh has made every reasonable effort to ensure that Edinburgh Research Explorer content complies with UK legislation. If you believe that the display of this file breaches copyright please contact openaccess@ed.ac.uk providing details, and we will remove access to the work immediately and investigate your claim.

Download date: 19. May. 2024

NOTICE: this is the author's version of a work that was accepted for publication in Sensors and Actuators A: Physical. Changes resulting from the publishing process, such as peer review, editing, corrections, structural formatting, and other quality control mechanisms may not be reflected in this document. Changes may have been made to this work since it was submitted for publication. A definitive version was subsequently published in Sensors and Actuators A: Physical, [VOL 226, PP. 149-153, (2015)] DOI:10.1016/j.sna.2015.02.023

Widely Tunable MEMS Ring Resonator with Electrothermal Actuation and Piezoelectric Sensing for Filtering Applications

Boris Sviličić[a,b,*], Enrico Mastropaolo[a], Rebecca Cheung[a]

[a]Scottish Microelectronics Centre, University of Edinburgh, EH9 3JF, United Kingdom

[b]Faculty of Maritime Studies, University of Rijeka, Studentska ulica 2, 51000, Croatia

[*]Corresponding author. Tel.: +385992116639; fax: +3855133675. Email: svilicic@pfri.hr

Abstract

In this paper, we present the design, fabrication and testing of two-port ring microelectromechanical (MEMS) resonant devices with electrothermal actuation and piezoelectric sensing for wide tunable filter applications. The ring resonators have been fabricated in silicon carbide with top platinum electrothermal actuator and lead zirconium titanate piezoelectric sensor. The two-port transmission frequency response measurements have shown that the devices with a ring radius between 125 µm and 200 µm resonate in the frequency range 0.4 MHz – 1.3 MHz, in the presence of tuning. By applying DC bias voltage in the range 4 V – 10 V, a frequency tuning range of 330,000 ppm has been achieved. Devices of similar design but with longer ring radius, actuated under the same operating conditions, have shown a wider frequency tuning range.

Keywords: MEMS resonator, tunable filter, electrothermal actuation, piezoelectric sensing

1. INTRODUCTION

Electrically tunable filters with a wide tunable range are key components in both multiband communication systems and wideband tracking receivers, as they possess the ability to replace filter banks [1-3]. Micro-electro-mechanical system (MEMS) resonators, for the past decade and so, have been extensively studied as a potential candidate technology for realization of a variety of devices including filters and frequency references [4,5]. Tunable filters based on MEMS resonator technology provide the ability to create low power frequency tuning with high Q factor while simultaneously reducing parts count, size, weight and price [6-9].

The leading techniques for electrical actuation and sensing of mechanical vibrations in MEMS resonators are electrostatic and piezoelectric transductions. Both techniques can be used for actuation and at the same time for tuning the resonant frequency by application of a DC bias voltage. Wide range resonant frequency tuning offered by electrostatic actuation technique is challenged by the trade-off between high DC bias voltages and complex fabrication process related to the small electrode-to-resonator gap spacing, while piezoelectric actuation technique provides fine resonant frequency tuning [10,11] and can be used to overcome fabrication tolerances and reliability issues. Electrothermal actuation, on the other hand, is an emerging technique that brings advantages such as simple fabrication process, low actuation voltages, impedance matching and wide frequency tuning range that can be obtained by applying low DC bias voltages [12-16].

Selection of the overall structural design of a resonator plays a very important role in achieving optimal performance of flexural-mode resonators. A ring structure can

achieve higher resonant frequency and larger quality factors compared to a beam structure thus motivating its usage for the MEMS resonators presented in this paper. Recently, we have demonstrated the fabrication of bimaterial (platinum and silicon carbide) ring structure and its operation as electrothermally actuated MEMS resonator has been detected optically [17]. Moreover, we have demonstrated the piezoelectric sensing of electrothermally actuated double-clamped beam MEMS resonators [18,19]. The use of piezoelectric transduction for electrical sensing allows active generation of electrical potential in response to an applied mechanical stress, and thus obviating the need of external bias voltage source, which is instead necessary for piezoresistive and capacitive transductions. In addition, piezoelectric transduction offers stronger electromechanical coupling, better impedance matching and relatively simpler fabrication compared to electrostatic transduction [20].

In this paper, we report on the design, fabrication and testing of electrothermally actuated flexural-mode ring resonators with piezoelectric read-out (Figure 1). In addition to the actuation function, electrothermal transduction has been used to tune the devices' resonant frequency in order to provide the wide tuning requirements and to compensate for frequency shifts due to changes in the operating conditions or by fabrication process imperfections. The design and position of the actuator (input port) and sensor (output port) have been optimized to achieve effective electrothermal actuation and high piezoelectric sensing respectively. Resonant behavior has been studied by performing two-port measurements of devices' transmission frequency response. The influence of the tuning DC bias voltage on the resonant frequency, Q factor and motional resistance,

Sensors and Actuators A: Physical, Volume 226, 2014, Pages 149–153, doi:10.1016/j.sna.2015.02.023

including the impact of ring dimensions on the resonant frequency tuning range, has been investigated.

2. PRINCIPLES OF OPERATION

Electrothermal actuation technique exploits the thermal expansion of a material as a driving force. In general, electrothermal resonant structures are composed of two layers of materials with different thermal expansion coefficients, so that one layer is used as actuation electrode and the other as one is used as resonant layer to be actuated. By applying a voltage across the electrothermal actuation electrode, Joule heating is generated and thereby a temperature gradient within the structure, leading to the thermal expansion of the entire structure and therefore to a mechanical strain. Electrothermal actuation can be obtained if the electrical power dissipated contains a frequency component equal to a structure's natural frequency f_0. Owing to the quadratic proportionality of the power on the driving voltage, the application of an actuation voltage with only AC component and the frequency f_{AC} can drive a device into resonance if the value of f_{AC} is equal to the half of the structure's natural frequency f_0 (f_{AC}=f_0/2) [17]. In order to drive a device into resonance using the actuation frequency equal to the structure's natural frequency (f_{AC}=f_0), the actuation signal should contain both AC and DC components. The generated thermal power is given by:

$$P = \frac{1}{R} \cdot \left(V_{DC}^2 + \frac{1}{2} V_{AC}^2 + 2 V_{DC} V_{AC} \sin \omega t + \frac{1}{2} V_{AC}^2 \sin 2\omega t \right) \quad (1)$$

$$= P_{stat} + P_{dyn1} \sin \omega t + P_{dyn2} \sin 2\omega t$$

Sensors and Actuators A: Physical, Volume 226, 2014, Pages 149–153, doi:10.1016/j.sna.2015.02.023

where R is the actuator resistance and ω is the angular frequency of the applied V_{AC}. The thermal power consists of the static component P_{stat} and two dynamic components P_{dyn1} and P_{dyn2}. The static component P_{stat} will result in a static temperature distribution through the structure, while the resonance will be achieved via the dynamic component P_{dyn1}.

Piezoelectric transduction has been used for electrical sensing of the structure's operation. Piezoelectricity refers to the ability of a material to generate an electrical potential actively when subjected to mechanical strain. In our devices, the piezoelectric layer is placed on the top of the main structure which, vibrates in vertical direction. As a consequence of the induced mechanical strain caused by the vibration, an alternating voltage with a frequency equal to the frequency of the mechanical vibrations can be detected.

3. EXPERIMENTAL DETAILS

3.1. Device design

The device has been designed as a two-port vertical-mode ring resonator (Figure 1). Cubic silicon carbide (3C-SiC) has been chosen as structural material due to its excellent mechanical properties that allow 3C-SiC resonators to achieve higher resonant frequencies compared to equivalent silicon (Si) resonators [21]. In addition, high thermal conductivity makes it particularly suitable for electrothermal actuation. The electrothermal actuator and piezoelectric sensor are placed on top of the ring for respectively actuating and sensing the vertical modes of the structure. The electrothermal actuator (input port) is formed from thin platinum (Pt) layer and it has been designed with

two Pt arms (the arms' width is 10 μm) connected by a perpendicular arm (u-shaped layout). The actuator is placed close to the hole in order to maximize vibration amplitude induced by heating and enhanced by the difference of the two materials' (Pt and 3C-SiC) thermal expansion coefficient [22,23]. The piezoelectric sensor is formed of a lead zirconium titanate (PZT) layer sandwiched between two Pt layers. The piezoelectric sensor has been designed to surround the hole and the actuator, as the induced vibration amplitude is the highest close to the center of the ring. PZT has been used due to its high piezoelectric coefficient, so that the electromechanical coupling is enhanced [20]. Figure 2 shows the top view schematics of the designed devices.

3.2. Fabrication

The devices have been fabricated with a ring radius of 125 μm, 170 μm and 200 μm and hole radius of 10 μm. The fabrication process consists of three main steps: all layers deposition, ports forming and the ring forming (Figure 3). A 2 μm thick 3C–SiC epilayer has been grown on 4-inch Si wafer, followed by the deposition of 100-nm-thick silicon dioxide (SiO_2) passivation layer and 10-nm-thick titanium (Ti) adhesion layer. The Pt/PZT/Pt stack has been deposited with thicknesses of 100/500/100 nm respectively. The ports have been defined photolithographically. The Pt and Ti layers have been dry etched while the PZT has been wet etched. The hole shape has been patterned photolithographically and the 3C-SiC layer through-etching to release the ring has been performed with inductively coupled plasma. Afterwards, the release of the Si sacrificial layer has been performed with a XeF_2 chemical etching. The detailed fabrication process for the Pt/PZT/Pt/Ti/3C-SiC ring structure is reported elsewhere [23].

3.3. Electrical characterization setup

Electrical characterization of the devices has been performed using an HP 8753C vector network analyzer. The devices under test have been directly connected to the network analyzer without the need for any external interface electronics. Signal-ground radio-frequency probes have been used and two-port short-open-load-through calibration has been performed before starting the measurements. In order to perform electrothermal actuation and resonant frequency tuning, the input AC signal provided with the network analyzer has been superimposed to a DC voltage provided by an additional stabilized DC source. The output signal has been taken from the top metal contact of the piezoelectric sensor, while the bottom metal contact has been grounded. The devices were exanimated in air, at room temperature and atmospheric pressure.

4. MEASUREMENT RESULTS AND DISCUSSION

Figure 4 shows the magnitude of transmission frequency response of the device with the 200 μm ring radius actuated with the input AC signal power of 10 dBm and DC voltage of 8 V. A resonant peak has been measured at 497.5 kHz with a quality (Q) factor in air of 160 for a thermal static power P_{stat} of 1.63 W and dynamic P_{dyn1} of 0.23 W. Tuning of the resonant frequency has been performed electrothermally by varying the input DC voltage. Figure 5 shows the resonant frequency shift measured at different DC voltages with AC input power equal to 10 dBm. As the DC tuning voltage increases from 4 V to 10 V, the resonant frequency decreases by -330,000 ppm (from 0.6 MHz to 0.4

MHz) thus indicating a relatively wide tuning capability. The decrease in resonant frequency detected as the DC tuning voltage increases can be explained by an increase of compressive stress in the ring, which is caused by the increase in thermal expansion of the structure as the temperature increases [16-18]. The inset of the Figure 5 shows the magnitude of transmission frequency response of the device actuated with the input signal power of 10 dBm and the maximal DC voltage of 10 V. It can be noted from the inset that the transmission magnitude curve is not distorted, indicating good linearity and power handling capacity of the device even at the highest tuning DC voltage of 10 V. However, by applying the AC input power higher than 10 dBm, the power handling capability of the device can be exceeded, which can be seen in the transmission magnitude curve distortion in Figure 6. The observed good linear behavior corresponds to our previous findings with the electrothermally actuated [18] and piezoelectrically transduced 3C-SiC resonators [11,23]. The most important aspect of the obtained results is that by using electrothermal tuning the operating frequency can be adjusted up to 33% of the un-tuned resonant frequency.

The presence of the DC tuning voltage in addition to the actuation AC signal has been found to affect the Q factor. Figure 7 shows the Q factor in air as a function of applied DC tuning voltage. The Q factor has been extracted from the transmission magnitude plots by calculating the ratio of the resonant frequency and the bandwidth of 3 dB transmission magnitude drop. The tested device have been actuated with a constant input AC signal power of 10 dBm while the DC tuning voltage has been swept in the range of 4 V - 10 V with step of 1 V. With the increase of DC tuning voltage, the Q factor in air has been observed to increase. In particular, as the DC tuning voltage is

Sensors and Actuators A: Physical, Volume 226, 2014, Pages 149–153, doi:10.1016/j.sna.2015.02.023

increased from 4 V to 6 V, the Q factor increases from ~85 to ~145. However, for the DC tuning voltages higher than 6 V, the Q factor value increase saturates, indicating constant bandwidth. It is worth pointing out that as the DC tuning voltage increases the Q factor has been observed to increase despite the decrease of resonant frequency. As the Q factor is defined by the ratio between the stored energy and the dissipated energy of a device per cycle of vibration, the heat generated as DC tuning voltage increases could cause an imbalance of the ratio thus leading to the observed Q factor increase. The Q factor could also be increased by reducing the piezoelectric sensor area covering the ring because the reduction of effective mass loading held by the ring should lead to lower dissipated energy [19]. It should be mentioned that measurements performed in vacuum conditions should give significantly higher values for the Q factor as the energy loss effect of air damping on the operation of our vertical-mode resonators would be reduced substantially [24]. In addition, operation in the vacuum condition, under the same actuation conditions, most probably would result in reduction of the resonant frequency and widening of the frequency tuning range [25,26].

The motional resistance dependence on the DC tuning voltage is shown in Figure 7, indicating a decrease of the motional resistance as the DC tuning voltage increases. The value of the equivalent motional resistance of the device, which has been directly connected to 50 Ω input and output impedance of the network analyzer, has been extracted from the transmission frequency response plots using the expression:

$$R_M = 2R_L \cdot \left(10^{-\frac{IL}{20}} - 1\right) \qquad (2)$$

Sensors and Actuators A: Physical, Volume 226, 2014, Pages 149–153, doi:10.1016/j.sna.2015.02.023

where R_M is the equivalent motional resistance, R_L is the source and load resistance of the network analyzer (both 50 Ω), and IL is the measured insertion loss of the device at its resonant frequency. With the DC tuning voltage increase from 4 V to 10 V, the motional resistance decreases from ~550 kΩ to ~180 kΩ. In addition, from Figure 7 it can be observed that the motional resistance decreases with a corresponding increase in Q factor. The motional resistance decrease with the increase of the DC tuning voltage can be attributed to stronger electromechanical coupling. With the increase of the DC tuning voltage, the thermally generated mechanical force increases and consequently the resonator vibration amplitude increases resulting in larger output signal [12].

The frequency tuning range has been found to be affected by the change of the ring radius. Figure 8 shows the frequency tuning characteristics of devices with ring radius of 125 μm and 170 μm together with the frequency tuning characteristics of the 200 μm device previously given in Figure 5. The tested devices differ only in the ring radius length, while other dimensions and technological parameters are the same. In order to perform a comparative study, the devices have been taken from the same wafer (fabrication related differences have been minimized) and tested in the same operating conditions. For DC tuning voltage in the range 4 V – 10 V, devices with ring radius of 125 μm and 170 μm resonates in frequency range 1 MHz - 1.3 MHz (frequency tuning range of ~230,00 ppm) and 0.56 MHz - 0.76 MHz (frequency tuning range of ~260,00 ppm) respectively. From figure 8, it can be observed that a wider tuning range can be achieved with devices with larger radius. In addition, for DC tuning voltage greater than 6 V, the frequency shift, as the voltage increases, becomes wider for devices with longer ring radius. The difference in the resonant frequency shift progressively increases with

the DC bias voltage increase. In particular, as the ring radius length increases from 125 μm to 200 μm, the frequency shift has been observed to increase from ~-55,000 ppm to ~-105,000 (frequency shift decrease of ~50,000 ppm) at DC bias voltage of 7 V and from ~-230,000 ppm to ~-330,000 (frequency shift increase of ~100,000 ppm) at DC bias voltage of 10 V. The wider resonant frequency tuning range obtained with the devices with longer ring radius can be explained by the larger influence of compressive stress. With the increase of the ring radius, the effective area of the ring increases, thus resulting in stronger influence of compressive stress in the ring compared to the devices with shorter ring radius. Moreover, as the DC tuning voltage increases, the induced temperature and the thermal expansion effect increase resulting in an additional increase of compressive stress and consequently in a larger decrease in resonant frequency of the devices with longer ring radius.

5. CONCLUSIONS

The integration of piezoelectric sensor on a ring MEMS resonator with electrothermal actuation has been demonstrated. The Pt electrothermal actuator (input port) and PZT piezoelectric sensor (output port) have been integrated on the top of 3C-SiC ring, forming a two-port vertical-mode resonator. The design of the actuator and the sensor is optimized to achieve effective electrothermal actuation and high piezoelectric output respectively. The resonant frequency tuning range up to ~330,000 ppm has been achieved using relatively low DC tuning voltage (4 V – 10 V). The detected decrease in resonant frequency is attributed to the increase of compressive stress in the ring. The detected decrease in resonant frequency is attributed to the increase of compressive stress

in the ring, while the change of motional resistance with the tuning DC voltage change is attributed to the change of the electromechanical coupling. Moreover, the frequency tuning range has been shown to be affected by the ring dimensions. With the increase of ring radius length, a wider frequency tuning range has been obtained probably due to larger compressive stress induced in the ring. The presented MEMS resonant devices show high resonant frequencies for given dimensions and wide resonant frequency tuning range with low DC bias voltages, which makes them promising candidates for use in filtering applications with wide frequency tuning requirement.

ACKNOWLEDGMENTS

One of us, B. Sviličić, acknowledges financial support of the Croatian Science Foundation and the University of Rijeka (grant 13.07.1.4.01).

References

[1] P. W. Wong, I. Hunter, Electronically tunable filters, IEEE Microwave Magazine 10 (2009) 46–54.

[2] G.M. Rebeiz, K. Entesari, I. Reines, S.J. Park, M.A. El-Tanani, A. Grichener, A.R. Brown, Tuning in to RF MEMS, IEEE Microwave Magazine 10 (2009) 55-72.

[3] R.R. Mansour, H. Fengxi, S. Fouladi, W.D. Yan, M. Nasr, High-Q Tunable Filters: Challenges and Potential, IEEE Microwave Magazine 15 (2014) 70-82.

[4] J.T.M. van Beek, R. Puers, A review of MEMS oscillators for frequency reference and timing applications, J. Micromech. Microeng., 22 (2012) 013001-35.

[5] C.T.C. Nguyen, MEMS Technology for Timing and Frequency Control, IEEE Trans. Ultrason. Ferroelectr. Freq. Control 54 (2007) 251-270.

[6] S.S. Li, Advances of CMOS-MEMS technology for resonator applications, IEEE Int. Conf. on Nano/Micro Engineered and Molecular Systems, 2013, 520-523.

[7] J.L. Lopez, J. Verd, A. Uranga, J. Giner, G. Murillo, F. Torres, G. Abadal, N. Barniol, A CMOS–MEMS RF-tunable bandpass filter based on two high-Q 22-MHz polysilicon clamped-clamped beam resonators, IEEE Electron Device Lett. 30 (2009) 718–720.

[8] G. Piazza, R. Abdolvand, G.K. Ho, F. Ayazi, Voltage-tunable piezoelectrically-transduced single-crystal silicon micromechanical resonators, Sens. Actuators A 111 (2004) 71–78.

[9] J. Giner, A. Uranga, F. Torres, E. Marigo , N. Barniol, Fully CMOS integrated bandpass filter based on mechanical coupling of two RF MEMS resonators, Electronics Lett. 46 (2010) 640-641.

[10] H. Chandrahalim, S.A. Bhave, R. Polcawich, J. Pulskamp, D. Judy, R. Kaul, M. Dubey, Performance comparison of $Pb(Zr_{0.52}Ti_{0.48})O_3$-only and $Pb(Zr_{0.52}Ti_{0.48})O_3$-on-silicon resonators, Appl. Phys. Lett. 93 (2008) 233504-233504-3.

[11] B. Sviličić, E. Mastropaolo, T. Chen, and R. Cheung, Piezoelectrically Transduced Silicon Carbide MEMS Double-Clamped Beam Resonators, J. of Vacuum Science and Technology B 30 (2012) 06FD05-1- 06FD05-7.

[12] A. Rahafrooz, S. Pourkamali, High-Frequency Thermally Actuated Electromechanical Resonators With Piezoresistive Readout, IEEE Trans. Electron Devices 58 (2011) 1205–1214.

[13] R.B. Reichenbach, M. Zalalutdinov, J.M. Parpia, H.G. Craighead, RF MEMS Oscillator with Integrated Resistive Transduction, IEEE Electron Device Lett. 27 (2006) 805–807.

[14] J.H. Seo, O. Brand, High Q-Factor In-Plane-Mode Resonant Microsensor Platform for Gaseous/Liquid Environment, J. Microelectromech. Syst. 17 (2008) 483–493.

[15] W. Zhanga, J.E.Y. Lee, Characterization and modeling of electro-thermal frequency tuning in a mechanical resonator with integral crossbar heaters, Sens. Actuators A 202 (2013) 69–74.

[16] C.S. Jun, X.M.H. Huang, M. Manolidis, C.A. Zorman, M. Mehregany, J. Hone, Electrothermal tuning of Al SiC nanomechanical resonators, Nanotechnology 17, (2006) 1506-1511.

[17] E. Mastropaolo, G.S. Wood, I. Gual, P. Parmiter, R. Cheung, Electrothermally Actuated Silicon Carbide Tunable MEMS Resonators, J. Microelectromech. Syst. 21 (2012) 811-821.

[18] B. Sviličić, E. Mastropaolo, B. Flynn, R. Cheung, Electrothermally Actuated and Piezoelectrically Sensed Silicon Carbide Tunable MEMS Resonator, IEEE Electron Device Lett. 33 (2012) 278-280.

[19] B. Sviličić, E. Mastropaolo, R. Cheung, Piezoelectric sensing of electrothermally actuated silicon carbide MEMS resonators, Microelectron. Eng. 119 (2014) 24-27.

[20] D.L. DeVoe, Piezoelectric thin film micromechanical beam resonators, Sens. Actuators A 88 (2001) 263-272.

[21] M. Placidia, P. Godignona, N. Mestresa, G. Abadalb, G. Ferroc, A. Leycurasd, T. Chassagne, Fabrication of monocrystalline 3C–SiC resonators for MHz frequency sensors applications, Sens. Actuat. B 133 (2008) 276–280.

[22] P. Srinivasan, M. Spearing, Effect of Heat Transfer on Materials Selection for Bimaterial Electrothermal Actuators, J. Microelectromech. Syst. 17 (2008) 653–667.

[23] E. Mastropaolo, B. Sviličić, T. Chen, B. Flynn, R. Cheung, Piezo-electrically actuated and sensed silicon carbide ring resonators, Microelectron. Eng. 97 (2012) 220-222.

[24] F. R. Blom, S. Bouwstra, M. Elwenspoek, J. H. J. Fluitman, Dependence of the quality factor of micromachined silicon beam resonators on pressure and geometry, J. of Vacuum Science and Technology B 10 (1992) 19 – 26.

[25] A. Rahafrooz, A. Hajjam, B. Tousifar, S. Pourkamali, Thermal actuation, a suitable mechanism for high frequency electromechanical resonators, IEEE Int. Conf. on Micro Electro Mechanical Systems, 2010, 200-203.

[26] H.J. Hall, A. Rahafrooz, J.J. Brown, V.M. Bright, S. Pourkamali, Thermally actuated I-shaped electromechanical VHF resonators, IEEE Int. Conf. on Micro Electro Mechanical Systems, 2012, 737-740.

Figure Captions

Figure 1. Optical micrograph of the one of the fabricated MEMS resonators with the electrothermal actuator (input port) and piezoelectric sensor (output port) placed on the top of the ring.

Figure 2. Top view schematics of the designed devices.

Figure 3. Fabrication process flow of the fabricated devices.

Figure 4. Two-port measurement of the transmission frequency response for the electrothermally actuated device with the ring radius of 200 μm using the input AC signal power of 10 dBm and DC bias voltage of 8 V.

Figure 5. Measured resonant frequency shift of the device with the ring radius of 200 μm versus DC tuning voltage. The inset shows transmission magnitude plot for applied input AC signal power of 10 dBm and DC bias voltage of 10 V.

Figure 6. Transmission magnitude plots for the device actuated using the input AC signal power of 15 dBm and 20 dBm and DC bias voltage of 10 V.

Figure 7. Measured Q factor in air and motional resistance of the device with the ring radius of 200 μm versus DC tuning voltage.

Figure 8. Measured resonant frequency shift versus DC bias voltage with ring radius R as a parameter.

Sensors and Actuators A: Physical, Volume 226, 2014, Pages 149–153, doi:10.1016/j.sna.2015.02.023

Figures

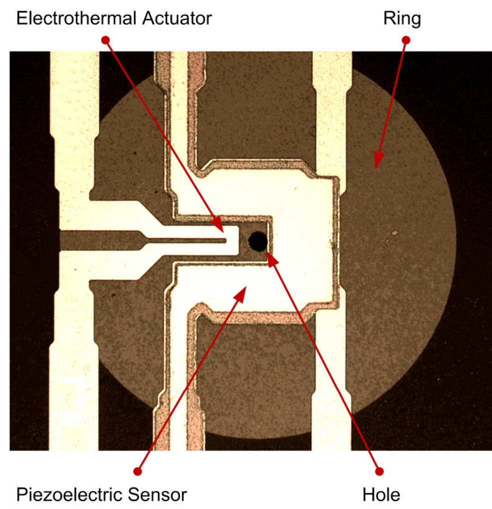

Figure 1

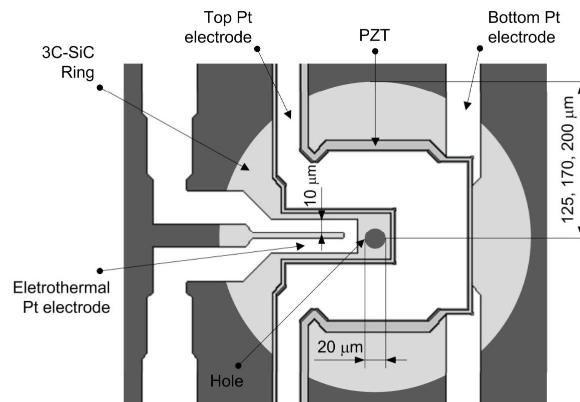

Figure 2

Sensors and Actuators A: Physical, Volume 226, 2014, Pages 149–153, doi:10.1016/j.sna.2015.02.023

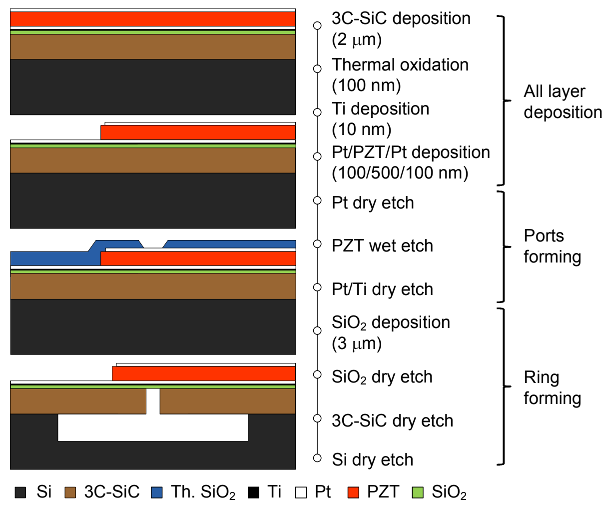

Figure 3

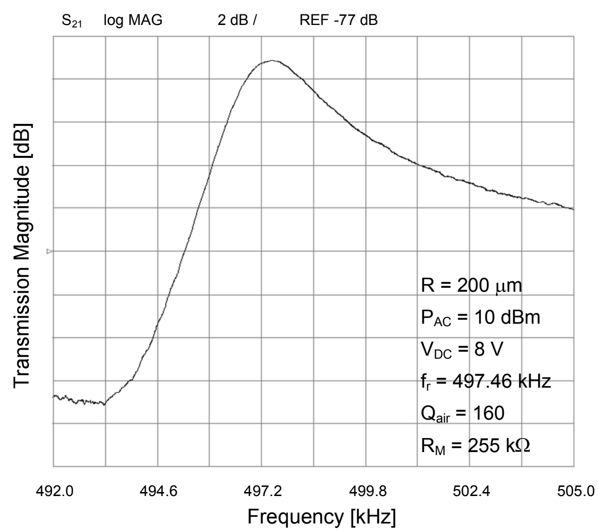

Figure 4

Sensors and Actuators A: Physical, Volume 226, 2014, Pages 149–153, doi:10.1016/j.sna.2015.02.023

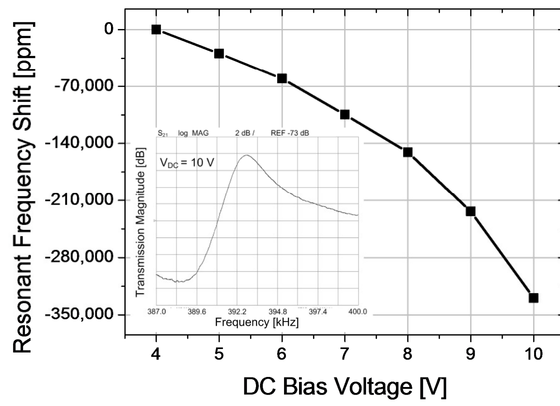

Figure 5

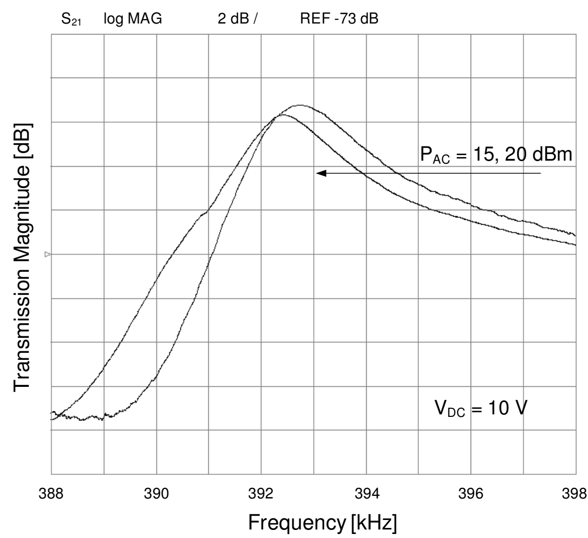

Figure 6

Sensors and Actuators A: Physical, Volume 226, 2014, Pages 149–153, doi:10.1016/j.sna.2015.02.023

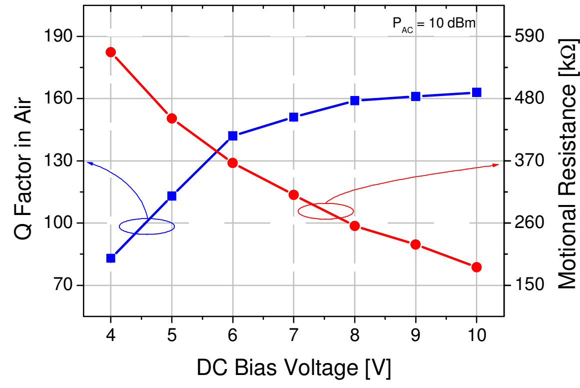

Figure 7

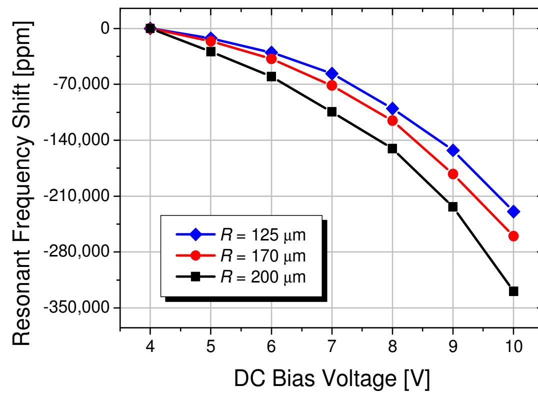

Figure 8

Vitae

Boris Sviličić received the diploma in electrical engineering (5 year curricula) from the Faculty of Electrical Engineering and Computing, University of Zagreb in 1999. Master of science and doctorate of science degrees in electrical engineering he received from the same institution in 2003 and 2008 respectively. He is currently an Associate Professor with the Faculty of Maritime Studies, University of Rijeka. His research interests involve design, simulation, fabrication and characterization of MEMS resonators, and analytical modeling and simulation of novel CMOS devices based on silicon-on-insulator technology.

Enrico Mastropaolo received the *Laurea* degree in microelectronics engineering from the Univeristà degli Studi di Padova, Padova, Italy, in 2006, and the Ph.D. degree in microsystems and microfabrication from The University of Edinburgh, U.K., in 2011. He is currently a Lecturer with the Scottish Microelectronics Centre, Institute for Integrated Micro and Nano Systems, in the School of Engineering of The University of Edinburgh. His research interests include design, simulations, fabrication and characterization of microelectromechanical systems (MEMS) devices, transduction techniques, SiC as structural material for MEMS, and nanostructures embedment in MEMS.

Rebecca Cheung received first-class honours and Ph.D. degrees in electronics and electrical engineering from the University of Glasgow, Glasgow, U.K., in 1986 and 1990, respectively. She is currently a Chair in nanoelectronics with the School of Engineering,

The University of Edinburgh, Edinburgh, U.K, and an Honorary Professor with the School of Engineering and Physical Sciences, Heriot–Watt University, Edinburgh. She has an international reputation for her contribution to the development and application of micro- and nano-fabrication. More recently, her research focuses on microresonators and microelectromechanical systems.